Article

Study on the Optimization of the Preparation Process of ZM5 Magnesium Alloy Micro-Arc Oxidation Hard Ceramic Coatings and Coatings Properties

Bingchun Jiang [1,2] , Zejun Wen [2], Peiwen Wang [1], Xinting Huang [1], Xin Yang [1], Minghua Yuan [1] and Jianjun Xi [1,*]

1 School of Mechanical and Electrical Engineering, Guangdong University of Science and Technology, Dongguan 523083, China; jiangbingchun_2008@163.com (B.J.); 17825244707@163.com (P.W.); 13480058689@163.com (X.H.); 3230002360@student.must.edu.mo (X.Y.); 15879018326@163.com (M.Y.)
2 School of Mechanical and Electrical Engineering, Hunan University of Science and Technology, Xiangtan 411201, China; zjwen732@163.com
* Correspondence: xjj63@163.com

Abstract: Hard ceramic coatings were successfully prepared on the surface of ZM5 magnesium alloy by micro-arc oxidation (MAO) technology in silicate and aluminate electrolytes, respectively. The optimization of hard ceramic coatings prepared in these electrolyte systems was investigated through an orthogonal experimental design. The microstructure, elemental composition, phase composition, and tribological properties of the coatings were characterized by scanning electron microscopy (SEM), energy-dispersive X-ray spectroscopy (EDS), X-ray diffraction (XRD), and tribological testing equipment. The results show that the growth of the hard ceramic coatings is significantly influenced by the different electrolyte systems. Coatings prepared from both systems have shown good wear resistance, with the aluminate electrolyte system being superior to the silicate system in performance. The optimized formulation for the silicate electrolyte solution has been determined to be sodium silicate at 8 g/L, sodium dihydrogen phosphate at 0.2 g/L, sodium tetraborate at 2 g/L, and potassium hydroxide at 1 g/L. The optimized formulation for the aluminate electrolyte solution consists of sodium aluminate at 5 g/L, sodium fluoride at 3 g/L, sodium citrate at 3 g/L, and sodium hydroxide at 0.5 g/L.

Keywords: ZM5 magnesium alloy; micro-arc oxidation; process optimization; hard ceramic coating; ultra-anti-corrosion; tribology

1. Introduction

Magnesium (Mg) and its alloys have the advantages of low density, high specific strength, good electromagnetic shielding performance, etc., and have broad application prospects in various industries such as automotive, electronics, aviation, and aerospace [1–3]. Due to the poor corrosion resistance and low hardness of Mg and its alloys, its application in many fields is minimal. Common surface treatment technologies include micro-arc oxidation (MAO) [4,5], electroplating [6,7], thermal spraying [8,9], sol-gel [10], electrodeposition [11], and other technologies. Micro-arc oxidation (MAO) technology is one of the most effective surface treatment technologies to improve the surface hardness of light metal [12].

Micro-arc oxidation technology, also known as micro-plasma oxidation or anode spark deposition, is a surface treatment technology developed based on anodic oxidation technology. Its principle is characterized by the use of arc discharge to enhance and activate the reaction occurring on the anode to form a high-quality strengthened ceramic coating on the surface of the workpiece [13,14]. In this technology, the metal on the surface of the workpiece interacts with the electrolyte solution by applying a voltage to the workpiece through a unique micro-arc oxidation power supply to form a micro-arc discharge. Under the action of high temperature, electric field, and other factors, ceramic coating is formed

on the metal surface to achieve the purpose of surface strengthening of the workpiece. In recent years, MAO technology has been successfully utilized to produce protective coatings on the surface of magnesium and its alloys, significantly enhancing the surface properties by increasing their resistance to wear, corrosion, and insulation. This advancement opens up new possibilities for the application of magnesium and its alloys. Furthermore, the MAO method can also be applied to process other metals and alloys such as aluminum and its alloys [15], titanium and its alloys [16], zinc alloys [17], etc., each with unique properties and potential uses. In micro-arc oxidation technology, the selection and optimization of electrolytic liquid systems are essential to achieve the best effect of the micro-arc oxidation technology on magnesium alloy. By adjusting parameters such as the composition [18], concentration [19], temperature [20], and pH value of the electrolyte [21], the formation and performance of the coating during the MAO process can be effectively controlled to meet the needs of different application scenarios. The properties of coatings prepared on magnesium and its alloys largely depend on the electrolyte's composition.

Du et al. [22] used micro-arc oxidation to prepare continuous and uniform dense coating under three electrolyte systems. They found that the phases, hardnesses, and friction factors of the three MAO coatings were significantly different, with the MAO coating layer prepared in the aluminate system having the highest roughness and hardness and the best wear resistance. Wang et al. [23] found that the thickness of the layer obtained in the sodium silicate electrolyte system was thicker than that of the sodium aluminate system and that the electrochemical corrosion resistance of the ceramic coatings obtained was significantly better than that of the sodium aluminates system through the cross-sectional appearance of the ceramic coatings. Muhaffel et al. [24] found that MAO coatings synthesized in aluminate electrolyte could not protect the AZ91 magnesium alloy from wear in corrosive media (0.9 wt.% NaCl solution) well compared to the dry sliding condition. Adding a certain amount of Na3PO4 to the acid electrolyte improved the corrosion resistance of the micro-arc oxidation coating of AZ91 magnesium alloy. Dong et al. [25] found that the thickness of the coatings obtained in the sodium aluminate electrolyte system was thicker than that in the sodium silicate electrolyte system and the electrochemical resistance of the coatings produced was significantly better than that in the sodium aluminate electrolyte system. Li et al. [26] showed an increase in abrasion resistance of the alloy by micro-arc oxidation with increased cathodic voltage in silicate electrolytes.

By adjusting the composition ratio of different electrolytes to change the ceramic coating's phase structure and thickness, the ceramic coating's corrosion resistance and wear resistance can be further affected. In this experiment, ZM5 was used as the research material to conduct an in-depth study of its electrochemical behavior during MAO. Through orthogonal experiments, the process parameters, electrolyte formula, and process flow were further optimized and the hard ceramic coatings preparation formula of silicate and aluminate electrolyte solution was explored. The oxide layer with high strength and high corrosion performance was prepared, which verified the feasibility and superiority of MAO technology of magnesium alloy and improved the engineering application prospect of ZM5 magnesium alloy. It provides a scientific basis for further optimization of process parameters.

2. Materials and Methods

2.1. Experimental Material and Coatings Preparation

The experimental material was ZM5 magnesium alloy, which was purchased commercially, provided by Shanghai Xuansheng Metal Product Co., Ltd. (Shanghai, China). and the mass fraction of each chemical component was Al 1.4%~2.0%, Zn 1.8%~2.8%, Mn 0.5%–0.68%, Si 5.0%~7.0%, Cu 0.03%, and the margin was Mg. The heat treatment state is quenching and artificial aging and its mechanical properties σ_b is 128 MPa, δ is 2.3%, and H is 89 HV.

The sample size is Φ20 mm × 5 mm, the through hole of Φ3 is processed above the sample, and the sample is preground by 400#, 800#, 1200#, 1500#, and 2000# water scrub to remove the oxide layer on the surface of the sample. The sample is fastened with Φ3 aluminum wire and immersed in electrolyte. The other end is connected to the positive electrode of the

power supply and the negative electrode of the power supply is connected to stainless steel. The electrolytes are sodium silicate and sodium aluminate, two electrolytic liquid systems prepared with deionized water. The pH value is 8~12 at room temperature. A unique power supply for asymmetric bipolar pulse micro-arc oxidation was used in the experiment and the detailed parameters of the electrical parameters were set as shown in Table 1. The electrolyte temperature is controlled at 20~40 °C and the micro-arc oxidation time t is 90 min.

Table 1. Primary establishment of electrical parameters.

Argument	Value
power supply P (kW)	50
pulse waveform	rectangular wave
polarity	bipolar
output mode	constant current
forward current density $i^+ (A/dm^2)$	10
positive and negative pulse width ratio ε	1:1
pulse frequency f (Hz)	50
negative positive current density ratio J	1.3:1

2.2. Experimental Scheme Design

In this paper, the process optimization scheme of ZM5 magnesium alloy micro-arc oxidation hard ceramic coatings was designed for silicate and aluminate electrolytic liquid systems, respectively. An orthogonal experimental design was adopted and a four-factor and three-level orthogonal Table was selected. In the silicate system, the test factors were Na_2SiO_3 (2 g/L, 5 g/L and 8 g/L), Na_2HPO_4 (0.2 g/L, 0.4 g/L and 0.6 g/L), $Na_2B_4O_7$ (1 g/L, 2 g/L and 3 g/L), and KOH (0.5 g/L, 1.0 g/L and 1.5 g/L). In the aluminate system, the test factors were $NaAlO_2$ 2 g/L, 5 g/L and 8 g/L), NaF 2 g/L, 3 g/L and 4 g/L), $C_6H_5Na_3O_7$ 1 g/L, 2 g/L and 3 g/L), and KOH (0.5 g/L, 1.0 g/L and 1.5 g/L). All chemicals utilized in this study were supplied by Macklin (Shanghai, China). The orthogonal design test Table L9 (3^4) is selected and the L9 orthogonal test Tables of different electrolytic liquid systems are shown in Tables 2 and 3.

Table 2. Orthogonal experimental table $L_9(3^4)$ of silicate.

Number	Factor	A: Na_2SiO_3 (g/L)	B: Na_2HPO_4 (g/L)	C: $Na_2B_4O_7$ (g/L)	D: KOH (g/L)
1		2	0.2	1	1
2		2	0.6	2	1.5
3		2	0.4	3	0.5
4		5	0.6	1	0.5
5		5	0.4	2	1
6		5	0.2	3	1.5
7		8	0.4	1	1.5
8		8	0.2	2	0.5
9		8	0.6	3	1

Table 3. Orthogonal experimental table $L_9(3^4)$ of aluminum chloride.

Number	Factor	A: $NaAlO_2$ (g/L)	B: NaF (g/L)	C: $C_6H_5Na_3O_7$ (g/L)	D: KOH (g/L)
1		2	2	1	1
2		2	4	2	1.5
3		2	3	3	0.5
4		5	4	1	0.5
5		5	3	2	1
6		5	2	3	1.5
7		8	3	1	1.5
8		8	2	2	0.5
9		8	4	3	1

2.3. Performance Test and Tissue Observation

The thickness of hard ceramic coatings was measured by CTG-10 digital eddy current thickness gauge. The hardness of dense layer *H* of hard ceramic coatings was measured by an HVS-1000 digital microhardness tester, provided by Quan De Electronic Instrument Department (Xiameng, China). An HD-E808-60 salt spray testing machine, provided by Dongguan Haida Instrument Co. (Dongguan, China), was used for anti-corrosion rating *Q* and its standard was referred to the salt spray testing national standard GB/T2423.17 [27] rating judgment method. Precision balance is used to measure the ceramic coatings' wear capacity Δm and the Russian BPC-01 friction and wear testing machine, provided by Optimol Corporation (Ural, Russia), is used for hard ceramic coatings friction and wear test. The dual material is GCr15, the friction condition is dry friction, the relative sliding speed is 0.8m/s, and the radial load is 90N. DISCOVER X-ray diffractometer, S-4700 scanning electron microscope (SEM), provided by Bruker Physik-AG (Saarbrücken, Germany) and Hitachi Limited (Tokyo, Japan) respectively, and energy dispersive spectrometer (EDS) were used to test the phase and cross-section morphology of the ceramic coating.

3. Results and Analysis

3.1. Range Analysis and Optimization Results

Range analysis is used to optimize the level of each factor. The more significant the range is, the more substantial the influence of this factor on the test index [4]. The most critical difference indicates that among all the factors, this factor has a significant impact on the test index. This paper adopts the comprehensive balance method to optimize the analysis. Table 4 shows the orthogonal test results of the silicate system and aluminate system. Salt spray test rating *Q* and hard ceramic coatings thickness *h* were used as evaluation indexes. Tables 5 and 6 show the variance analysis results of salt corrosion resistance grade and ceramic coatings thickness index under silicate and aluminate electrolyte conditions, respectively. It can be judged that the optimal formula of silicate electrolyte is as follows: 8 g/L sodium silicate, 0.2 g/L disodium hydrogen phosphate, 2 g/L sodium tetraborate, and 1 g/L potassium hydroxide. The optimal formula of aluminate electrolyte is as follows: sodium aluminate 5 g/L, sodium fluoride 3 g/L, sodium citrate 3 g/L, and sodium hydroxide 0.5 g/L.

Table 4. Results of $L_9(3^4)$ orthogonal tests under different systems.

Number	Factor	Silicate System		Aluminate System	
		Q	*h* (μm)	*Q*	*h* (μm)
1		8	59	5	41
2		0	36	4	28
3		1	45	10	46
4		0	27	5	49
5		7	50	8	36
6		5	52	5	28
7		8	63	6	31
8		9	67	4	43
9		4	44	3	29

3.2. Effect of Two Electrolytic Liquid Systems on the Growth of Hard Ceramic Coatings

Figure 1 shows the concentration of sodium silicate and sodium aluminate, the fluctuation voltage (V_q) of micro-arc oxidation, and the hardness (*H*) of the coatings. V_q and *H* have the same trend with sodium silicate and sodium aluminate concentrations. As can be seen from Figure 1a, with the increase in sodium silicate and sodium aluminate concentrations, the corresponding fluctuating voltage decreases, which is caused by the rise in the conductivity of the electrolyte. When the concentration is 2 g/L, the fluctuation voltage of sodium aluminate electrolyte (475.3 V) is higher than that of sodium aluminate

electrolyte (416.9V). With the increase in sodium silicate and sodium aluminate concentration, the arc voltage of the sodium aluminate electrolyte system drops faster than that of the sodium silicate electrolyte system. When the concentration of the two electrolytes is less than 5 g/L, the V_q of sodium aluminate electrolyte is greater than that of sodium silicate electrolyte. The situation is reversed when the concentration of the two electrolytes is greater than 5 g/L. It can be shown that the growth of hard ceramic coatings of magnesium alloys is significantly affected by the concentration of different electrolytic liquid systems. It can be seen from Figure 1b that the coating hardness of ZM5 magnesium alloy prepared under the two electrolytic liquid systems is higher. The hardness of hard coatings increases with the increase in sodium silicate and sodium aluminate. When the concentration is 2 g/L, the hardness of sodium aluminate hard coatings (461.7 HV) is lower than that of sodium aluminate hard coatings (577.2 HV). With the increased concentration of sodium silicate and sodium aluminate, the rise rate of sodium hard coatings H prepared by sodium aluminate electrolytic liquid is faster than that of sodium silicate electrolytic liquid.

Table 5. Data processing results of silicate corrosion resistance grade and ceramic film thickness indicators.

	Index	Na_2SiO_3 (g/L)	Na_2HPO_4 (g/L)	$Na_2B_4O_7$ (g/L)	KOH (g/L)
	Q_1	9	22	16	10
	Q_2	12	16	16	19
	Q_3	21	4	10	13
	q_1	3	7.33	5.3	3.3
Q	q_2	4	5.33	5.3	6.3
	q_3	7	1.33	3.3	4.33
	extreme/q'	3	6	2	3
	optimized result	8	0.2	1 and 2	1
	h_1	46.7	59.3	49.67	46.33
	h_2	43	52.67	51	51
h (μm)	h_3	58	35.67	47	50.33
	extreme/h'	15	23.63	4	4.67
	optimized result	8	0.2	2	1

Table 6. Data processing results of aluminate corrosion resistance grade and ceramic film thickness indicators.

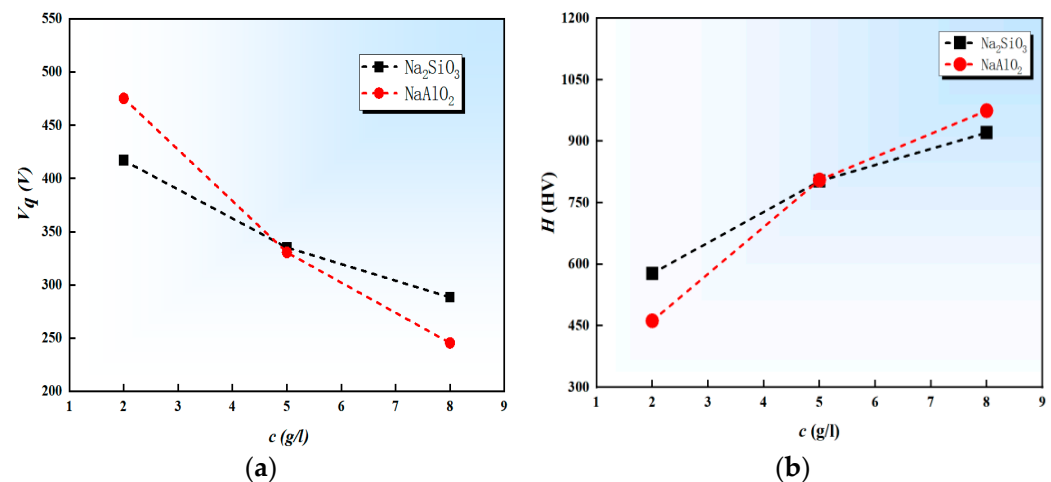|	Index	$NaAlO_2$ (g/L)	Na_2HPO_4 (g/L)	$Na_2B_4O_7$ (g/L)	KOH (g/L)
	Q_1	19	14	16	19
	Q_2	18	24	16	16
	Q_3	13	12	18	15
	q_1	6.33	4.67	5.33	6.33
Q	q_2	6	8	5.33	5.33
	q_3	4.33	4	6	5
	extreme/q'	2	4	0.67	1.33
	optimized result	5	3	3	0.5
	h_1	38.33	35.67	40.33	46
	h_2	37.67	37.33	35.67	35.33
h (μm)	h_3	34.33	37.67	34.33	29
	extreme/h'	4	2	6	17
	optimized result	5	3	1	0.5

Figure 1. The relationship between *Vq*, *H*, and *c* under different electrolytic liquid systems (**a**) *Vq-c*; (**b**) *H-c*.

When the concentration is 5 g/L, the hardness of the coatings is close. When the concentration reaches 8 g/L, the hardness of the coatings exceeds 800 HV. It is concluded that the growth of hard ceramic coatings of magnesium alloys is also significantly affected by the concentration of different electrolytic liquid systems. Studies in the literature [4–6] show that electrolyte concentration positively correlates with conductivity. When the conductivity of the electrolyte is too large, the instantaneous energy of discharge will cause breakdown and damage in the micro-melt zone of the breakdown discharge, increasing defects in the ceramic coatings [28,29]. Therefore, in preparing hard ceramic coatings by micro-arc oxidation on the surface of ZM5 magnesium alloy, the sodium aluminate electrolytic liquid system is better than the sodium silicate electrolytic liquid system. When the concentration of sodium aluminate is 5~8 g/L, the hard ceramic coatings with high hardness and tiny pores can be prepared.

Figure 2 shows the coating thickness and hardness of the hard coatings under different electrolytic liquid systems. It can be seen from Figure 2a that the thickness of the micro-arc oxidation coatings gradually increases with the extension of oxidation time. At first, the growth rate of the ceramic coatings was speedy and then gradually slowed down until the thickness of the ceramic coatings no longer increased and the growth and dissolution rate of the ceramic coatings reached a relative dynamic balance. When $t < 65$ min, the long coatings velocity of ceramic coatings in the sodium silicate electrolytic liquid system is higher than that in the sodium aluminate electrolytic liquid system. When $t > 65$ min, the situation was reversed. This phenomenon may be related to the activity of silicon and aluminum elements and their atomic groups in the electrolytic liquid system [30,31]. It can be seen from Figure 2b that the hardness of the ceramic coating increases with the thickening of the dense layer (h_1) and the wear resistance of the coatings is correspondingly improved. It can also be seen from the figure that when $h_1 > 35$ μm, the hardness of ceramic coatings prepared by sodium aluminate electrolyte system is higher than that of sodium silicate electrolyte system. It is found in the test that when the forward current density $i^+ < 5$ A/dm^2, the energy of the breakdown moment is small, the dense layer phase transition energy is insufficient, and the hardness is low.
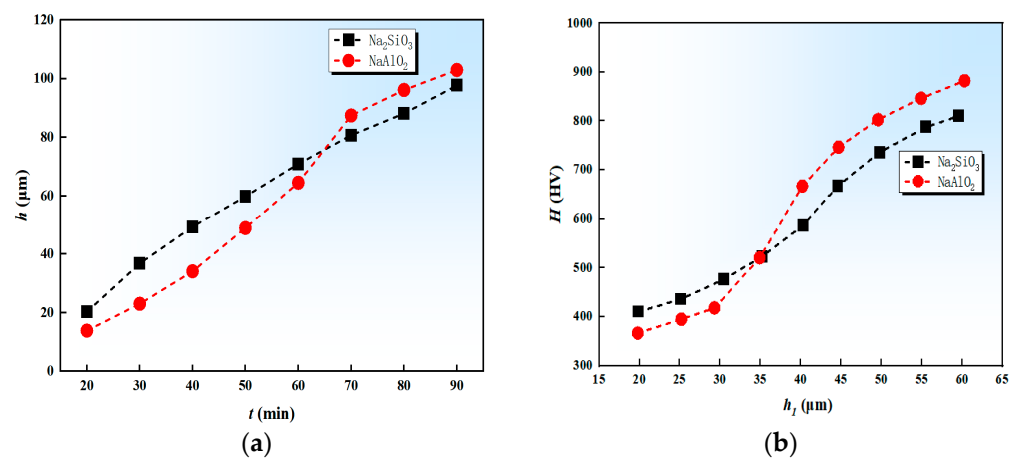
Figure 2. Coatings thickness and hardness of different electrolytic liquid systems: (**a**) *h-t* and (**b**) *H-h₁*.

3.3. Analysis of Hard Ceramic Coating Phase Structure and Profile Profile

Figure 3 shows the X-ray diffraction patterns of hard ceramic coatings prepared under different electrolytic liquid systems. As can be seen from Figure 3a, the compact layer of hard ceramic coatings prepared by the sodium silicate system is mainly composed of cube MgO and a small amount of spinel $MgAl_2O_4$, $MgSiO_3$, and Mg_2SiO_4. The main reaction equation is as follows:

$$Mg^{2+} + OH^- \rightarrow Mg(OH)_2 \rightarrow MgO + H_2O \tag{1}$$

$$Mg^{2+} + SiO_3^{2-} \rightarrow MgSiO_3 \tag{2}$$

$$2Mg^{2+} + SiO_3^{2-} + 2OH^- \rightarrow Mg_2SiO_4 + H_2O \tag{3}$$
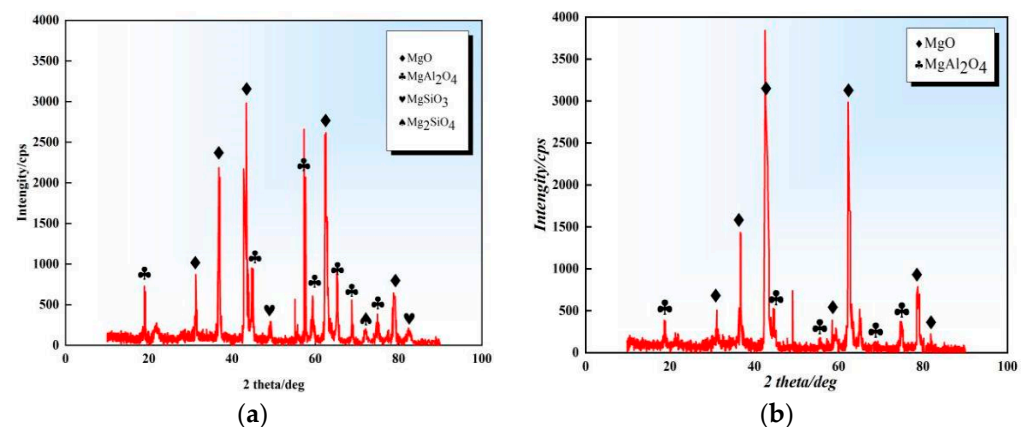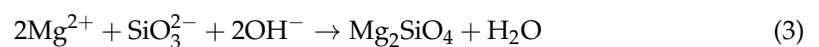
Figure 3. X-ray diffraction of hard ceramic coatings prepared with different electrolytic liquid systems: (**a**) silicate and (**b**) aluminates.

As shown in Figure 3b, the hard ceramic coatings prepared by the aluminate system mainly consist of cube MgO and spinel $MgAl_2O_4$. The primary reaction equation is as follows:

$$Mg^{2+} + OH^- \rightarrow Mg(OH)_2 \rightarrow MgO + H_2O \tag{4}$$

$$Mg^{2+} + 2AlO^- \rightarrow MgAl_2O_4 \tag{5}$$
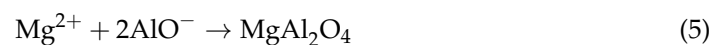
The hard coatings prepared by the two electrolytic liquid systems contains a MgO phase with a larger crystal size due to sufficient crystal growth. Its corrosion resistance is greatly improved, while the hard ceramic coatings generated by sodium aluminate system micro-arc oxidation have better corrosion resistance, mainly because its crystal structure

contains rich corrosion-resistant crystal—$MgAl_2O_4$. The properties of MAO ceramic coatings of magnesium alloys are significantly affected by the crystal phase. Specifically, the nature and dispersion pattern of the crystalline phase profoundly influence the microstructural organization and mechanical attributes of the coating, thereby exerting a significant impact on its corrosion resistance and mechanical robustness. In the MAO ceramic coating of magnesium alloy, the primary crystalline phase comprises oxides and the uniform dispersion of fine grains serves to enhance the density of the coating. Additionally, it enhanced the bonding strength between the oxide coatings and the substrate, ultimately increasing the corrosion resistance of the material.

Figure 4 shows the profile of the dense layer of hard ceramic coatings under different electrolytic liquid systems. It can be seen from the figure that the dense thickness of the hard coatings prepared by the silicate system and the aluminate system is ~69.6 μm and ~83.4 μm, accounting for 71.2% and 81.1% of the coatings' thickness, respectively. The density of the ceramic coatings prepared by the aluminate system is better than that of the silicate system and there is no obvious crack. In contrast, the ceramic coatings prepared by the silicate system have apparent cracks. This difference is mainly due to the high content of alumina in the aluminate system, which provides better thermal and chemical stability as well as better corrosion resistance. Moreover, during the preparation of the aluminate system, a layer of tightly bonded oxide layer was formed on the surface of aluminum oxide and magnesium alloy, which enhanced the adhesion and crack resistance of the coating.
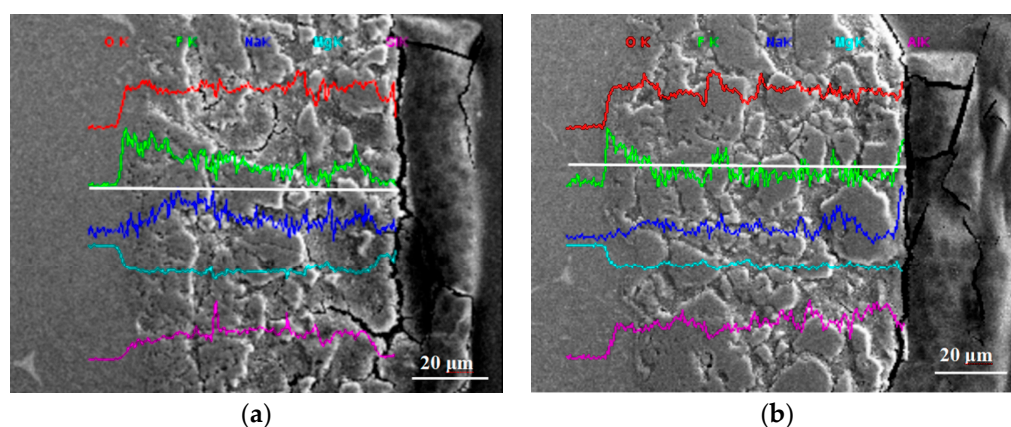

(a)　　　　　　　　　　　　　　　(b)

Figure 4. Cross-section topography and line analysis of hard ceramic coatings prepared with different electrolytic liquid systems: (**a**) silicate and (**b**) aluminates.

Figure 5 shows the corrosion resistance spectra of hard ceramic coatings prepared under different electrolytic liquid systems. It can be seen from Figure 5a that the elements contained in the hard ceramic coatings can be found in the electrolyte, among which the main elements are Mg, O, and Si, indicating that the main product of the corrosion-resistant hard ceramic coatings is MgO and $Mg_3[Si_4O_{10}](OH)_2$. As can be seen from Figure 5b, The crystal phase structure of the super anticorrosive coatings grown by MAO of aluminate electrolytic liquid system is mainly composed of MgO, Al_2O_3, and $MgAl_2O_4$ phases. Magnesium aluminum spinel ($MgAl_2O_4$) is a good performance of ceramic materials; its chemical properties are stable. When placed at room temperature, no acid or alkali reaction occurs and it has strong resistance to various melt erosion at high temperatures. Therefore, the MAO ceramic coating with Mg-Al spinel as the main phase has better corrosion resistance.
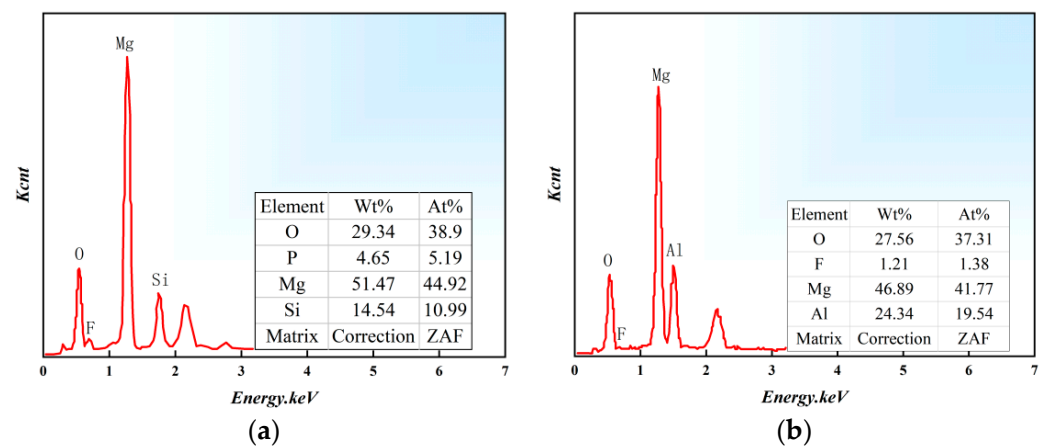
Figure 5. The energy spectrum of the sample of silicate system: (**a**) silicate and (**b**) aluminates.

3.4. Tribological Analysis of Hard Ceramic Coatings

The porous ceramic coatings generated by MAO can increase the contact area between the material and the surrounding environment, facilitate the diffusion of metal ions from the substrate, and further enhance corrosion resistance. This kind of ceramic coating has high hardness, good wear resistance, and corrosion resistance and can effectively resist friction and wear. Figures 6 and 7 show the relationship curves of wear quantity Δm—wear time t_m and μ—friction time t_c of ZM5 magnesium alloy micro-arc oxidation hard ceramic coatings, respectively. It can be seen from Figures 6 and 7 that Δm and μ decrease with the elongation of t_m and t_c because the generated ceramic coatings can be divided into a transition layer, dense layer, and loose layer from the inside out. The transition layer near the magnesium alloy matrix is metallurgically combined with the matrix. The dense layer mainly comprises MgO with good wear resistance and corrosion resistance, high hardness, and a small amount of $MgAl_2O_4$, Mg_2SiO_4, and $MgSiO_3$. The loose layer mainly comprises $MgAl_2O_4$, Mg_2SiO_4, and $MgSiO_3$ [32]. In addition, the microstructure and composition of ceramic coating grown on the MAO surface of magnesium alloy also have important effects on its wear resistance. The more uniform and dense the microstructure of the ceramic coating, the better the wear resistance. The tissue of the loose layer is loose so the wear amount and friction coefficient are significant. When the loose layer is removed, the wear amount begins to decrease gradually and the μ decreases accordingly and finally tends to be stable. The reason is that before 60 min, the loose layer of the ceramic coating gradually wears out. The decline rate of Δm and μ is fast, while after 60 min, the loose layer reaches the dense layer after wearing out and the density of the dense layer is improved and the hardness is increased, so the decline rate of Δm and μ becomes slow. The friction coefficient has a specific range for some commonly used wear-resistant materials, such as steel, plastics, rubber, etc. In these materials, the coefficient of friction below 0.3 is considered good tolerance. When the hard ceramic coating reaches 0.3, the coating time of the silicate system is about 20 min longer than that of the aluminate system. It can be inferred that the wear resistance of the loose layer of silicate coatings is more robust than that of the loose layer of aluminate coatings and the wear resistance of the dense layer of silicate coatings is more robust than that of the loose layer of aluminate coatings.
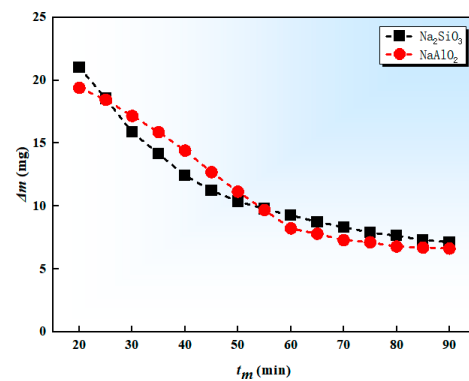
Figure 6. Relation between Δm and t_m.
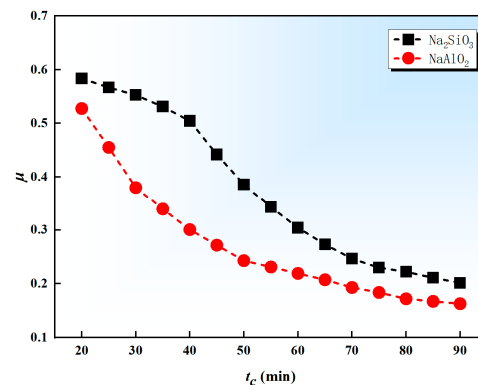

Figure 7. Relation between μ and t_c.

4. Conclusions

1. In preparing hard ceramic coatings by micro-arc oxidation on the surface of ZM5 magnesium alloy, the sodium aluminate electrolytic liquid system is better than the sodium silicate electrolytic liquid system. When the concentration of sodium aluminate is 5~8 g/L, the hard ceramic coatings with high hardness and tiny pores can be prepared;

2. The orthogonal experimental design method obtained the optimum process formula of micro-arc oxidation hard ceramic coatings under two systems. The optimal formula of silicate electrolyte is as follows: 8 g/L sodium silicate, 0.2 g/L disodium hydrogen phosphate, 2 g/L sodium tetraborate, and 1 g/L potassium hydroxide. The optimal formula of aluminate electrolyte is sodium aluminate 5 g/L, sodium fluoride 3 g/L, sodium citrate 3 g/L, and sodium hydroxide 0.5 g/L.

3. The coatings prepared by the two electrolytic liquid systems have good wear resistance. The wear resistance of the loose layer of silicate coatings is more robust than that of the loose layer of aluminate coatings and the wear resistance of the dense layer of silicate coatings is more robust than that of the dense layer of aluminate coatings.

Author Contributions: Conceptualization, B.J. and J.X.; methodology, B.J. and J.X.; validation, J.X. and Z.W.; formal analysis, B.J., P.W. and J.X.; investigation, P.W.; resources, B.J.; data curation, B.J., P.W., M.Y. and J.X.; writing—original draft preparation, B.J., P.W., X.H. and J.X.; writing—review and editing, B.J., Z.W., X.Y. and J.X.; visualization, X.H. and X.Y.; supervision, J.X.; project administration, B.J.; funding acquisition, B.J. and M.Y. All authors have read and agreed to the published version of the manuscript.

Data Availability Statement: The original contributions presented in the study are included in the article, further inquiries can be directed to the corresponding author.

Conflicts of Interest: The authors declare no conflict of interest.

References

1. Rao, Y.Q.; Wang, Q.; Chen, J.X.; Ramachandran, C.S. Abrasion, sliding wear, corrosion, and cavitation erosion characteristics of a duplex coating formed on AZ31 Mg alloy by sequential application of cold spray and plasma electrolytic oxidation techniques. *Mater. Commun.* **2021**, *26*, 101978. [CrossRef]
2. Chen, Y.N.; Wu, L.; Yao, W.H.; Zhong, Z.Y.; Chen, Y.H.; Wu, J.H.; Pan, F.S. One-step in situ synthesis of graphene oxide Mg/Al-layered double hydroxide coating on a micro-arc oxidation coating for enhanced corrosion protection of magnesium alloys. *Surf. Coat. Technol.* **2021**, *413*, 127083. [CrossRef]
3. Ly, X.N.; Yang, S.; Nguyen, T.H. Effect of equal channel angular pressing as the pretreatment on microstructure and corrosion behavior of micro-arc oxidation (MAO) composite coating on biodegradable Mg-Zn-Ca alloy. *Surf. Coat. Technol.* **2020**, *395*, 125923. [CrossRef]
4. Xue, K.; Tan, P.H.; Zhao, Z.H.; Cui, L.Y.; Kannan, M.B.; Li, S.Q.; Liu, C.B.; Zou, Y.H.; Zhang, F.; Chen, Z.Y.; et al. In vitro degradation and multi-antibacterial mechanisms of β-cyclodextrin@curcumin embodied $Mg(OH)_2$/MAO coating on AZ31 magnesium alloy. *J. Mater. Sci. Technol.* **2023**, *132*, 179–192. [CrossRef]
5. Xia, Q.X.; Li, X.; Yao, Z.P.; Jiang, Z.H. Investigations on the thermal control properties and corrosion resistance of MAO coatings prepared on Mg-5Y-7Gd-1Nd-0.5Zr alloy. *Surf. Coat. Technol.* **2021**, *409*, 126874. [CrossRef]
6. Singh, C.; Tiwari, S.K.; Singh, R. Development of corrosion-resistant electroplating on AZ91 Mg Alloy by employing air and water-stable eutectic based ionic liquid bath. *Surf. Coat. Technol.* **2021**, *428*, 127881. [CrossRef]
7. Meng, X.; Wang, J.L.; Zhang, J.; Niu, B.L.; Gao, X.H.; Yan, H. Electroplated super-hydrophobic Zn-Fe coating for corrosion protection on magnesium alloy. *Trans. Nonferrous Met. Soc. China* **2022**, *32*, 3250–3258. [CrossRef]
8. Marzbanrad, B.; Razmpoosh, M.H.; Toyserkanic, E.; Jahed, H. Role of heat balance on the microstructure evolution of cold spray coated AZ31B with AA7075. *J. Magnes. Alloys* **2021**, *9*, 1458–1469. [CrossRef]
9. Palanisamy, K.; Gangolu, S.; Antony, J.M. Effects of HVOF spray parameters on porosity and hardness of 316L SS coated Mg AZ80 alloy. *Surf. Coat. Technol.* **2022**, *448*, 128898. [CrossRef]
10. Pereira, G.S.; Ramirez, O.M.P.; Avila, P.R.T.; Avila, J.A.; Pinto, H.C.; Miyazaki, M.H.; De Melo, H.G.; Bose Filho, W. Cerium conversion coating and sol-gel coating for corrosion protection of The WE43 Mg alloy. *Corrfosion Sci.* **2022**, *206*, 110527. [CrossRef]
11. Fattah-Alhosseini, A.; Chaharmahali, R.; Babaei, K. Effect of particles addition to solution of plasma electrolytic oxidation (PEO) on the properties of PEO coatings formed on magnesium and its alloys, a review. *J. Magnes. Alloys* **2020**, *8*, 799–818. [CrossRef]
12. Chaharmahali, R.; Fattah-Alhosseini, A.; Babaei, K. Surface characterization and corrosion behavior of calcium phosphate (Ca-P) base composite layer on Mg and its alloys using plasma electrolytic oxidation (PEO): A review. *J. Magnes. Alloys* **2021**, *9*, 21–40. [CrossRef]
13. Kaseema, M.; Fatimah, S.; Nashrah, N.; Ko, Y.G. Recent progress in surface modification of metals coated by plasma electrolytic oxidation: Principle, structure, and performance. *Prog. Mater. Sci.* **2021**, *117*, 100735. [CrossRef]
14. Lin, Z.S.; Wang, T.L.; Yu, X.M.; Sun, X.T.; Yang, H.Z. Functionalization treatment of micro-arc oxidation coatings on magnesium alloys: A review. *J. Alloys Compd.* **2021**, *879*, 160453. [CrossRef]
15. Chen, X.Y.; Zhang, Z.Q.; Duan, Y.W.; Wang, X.D. Growth mechanism of 2024 aluminum alloy micro-arc oxide layer in cobalt-containing electrolyte. *Surf. Coat. Technol.* **2023**, *462*, 129461. [CrossRef]
16. Chwartz, A.; Kossenko, A.; Zinigrad, M.; Danchuk, V.; Sobolev, A. Cleaning strategies of synthesized bioactive coatings by PEO on Ti-6Al-4V alloys of organic contaminations. *Materials* **2023**, *16*, 4624. [CrossRef] [PubMed]
17. Wang, S.K.; Meng, J.B.; Guan, Q.Y.; Dong, X.J.; Yu, H.Y.; Li, H.M.; Li, L. Preparation and performance analysis of CeO_2 particle-doped micro-arc oxidized composite film layer on the surface of copper-zinc alloy. *Surf. Technol.* **2023**, *52*, 152–161. [CrossRef]
18. Wu, J.H.; Wu, L.; Yao, W.H.; Chen, Y.N.; Chen, Y.H.; Yuan, Y.; Wang, J.F.; Atrens, A.; Pan, F.S. Effect of electrolyte systems on plasma electrolytic oxidation coatings characteristics on LPSO Mg-Gd-Y-Zn alloy. *Surf. Coat. Technol.* **2023**, *454*, 129192. [CrossRef]
19. Xie, P.; Blawert, C.; Serdechnova, M.; Konchakova, N.; Shulha, T.; Wu, T.; Zheludkevich, M.L. Effect of low concentration electrolytes on the formation and corrosion resistance of PEO coatings on AM50 magnesium alloy. *J. Magnes. Alloys* **2024**, *12*, 1386–1405. [CrossRef]
20. Wang, J.; Lu, H.L.; Sun, Z.B.; Xu, G.S.; Bai, Z.D.; Peng, Z.J. Effect of ultra accurate control of electrolyte temperature on the performance of micro arc oxidation ceramic coatings. *Ceram. Int.* **2023**, *49*, 33236–33246. [CrossRef]

21. Yao, W.H.; Zhan, G.X.; Chen, Y.H.; Qin, J.; Wu, L.; Chen, Y.N.; Wu, J.H.; Jiang, B.; Atrens, A.; Pan, F.S. Influence of pH on corrosion resistance of slippery liquid-infused porous surface on magnesium alloy. *Ftransactions Nonferrous Met. Soc. China* **2023**, *33*, 3309–3318. [CrossRef]

22. Du, C.Y.; Huang, S.T.; Yang, H.C.; Hu, Y.H.; Yu, X.L. Microstructure and properties of micro-arc oxidation films on SiC/AI matrix composites in different electrolyte systems. *J. Mater. Eng.* **2023**, *51*, 139–149.

23. Wang, Z.Y.; Ma, Y.; An, S.J.; Sun, L. Effect of electrolyte formulation on the corrosion resistance of micro-arc oxidation coating of pure magnesium. *Mater. Rep.* **2023**, *37*, 173–182.

24. Muhaffel, F.; Cimenoglu, H. Development of corrosion and wear resistant micro-arc oxidation coating on a magnesium alloy. *Surf. Coat. Technol.* **2019**, *357*, 822–832. [CrossRef]

25. Dong, H.R.; Li, Q.; Xie, D.B.; Jiang, W.G.; Ding, H.J.; Wang, S.; An, L.Y. Forming characteristics and mechanisms of micro-arc oxidation coatings on magnesium alloys based on different types of single electrolyte solutions. *Ceram. Int.* **2023**, *49*, 32271–32281. [CrossRef]

26. Li, X.J.; Zhangm, M.; Wen, S.; Mao, X.; Huo, W.G.; Guo, Y.Y. Microstructure and wear resistance of micro-arc oxidation ceramic coatings prepared on 2A50 aluminum alloys. *Surf. Coat. Technol.* **2020**, *394*, 125853. [CrossRef]

27. *GB/T2423.17*; Environmental testing for electric and electronic products: Part 2: Test Methods-Test Ka: Salt Mist. National Standards of People's Republic of China: Beijing, China, 2008.

28. Feng, Y.R.; Zhou, L.; Jia, H.Y.; Zhang, X.; Zhao, L.B.; Fang, D.Q. Research progress on micro-arc oxidation of medical magnesium alloy. *Surf. Technol.* **2023**, *52*, 11–24. [CrossRef]

29. Chen, H.T.; Li, Z.S.; He, Q.B.; Wu, H.L.; Ma, Y.Z.; Li, L. Study on artificial neural network used for optimization of micro-arc oxidation of magnesium alloys. *Rare Met. Mater. Eng.* **2012**, *41*, 23–27.

30. Guo, H.F.; An, M.Z. Growth of ceramic coatings on AZ91D magnesium alloys by micro-arc oxidation in aluminate–fluoride solutions and evaluation of corrosion resistance. *Appl. Surf. Sci.* **2005**, *246*, 229–238. [CrossRef]

31. Jia, Q.R.; Cui, H.W.; Zhang, T.T.; Cui, X.L.; Pan, Y.K.; Feng, R. General situation on research of micro-arc oxidation technology of magnesium alloys. *Mater. Prot.* **2018**, *51*, 108–113. [CrossRef]

32. Ma, N.; Huang, J.M.; Su, J.; Yin, L.Y. Effects of MgO nanoparticles on corrosion and wear behavior of micro-arc oxide coatings formed on AZ31B magnesium alloy. *Mater. Rep.* **2018**, *32*, 2768–2772. [CrossRef]